THE JOURNAL OF PHYSICAL CHEMISTRY B

Article

pubs.acs.org/JPCB

pH-, Sugar-, and Temperature-Sensitive Electrochemical Switch Amplified by Enzymatic Reaction and Controlled by Logic Gates Based on Semi-Interpenetrating Polymer Networks

Dan Liu, Hongyun Liu, and Naifei Hu*

Department of Chemistry, Beijing Normal University, Beijing 100875, P. R. China

Supporting Information

ABSTRACT: Phenylboronic acid (PBA) moieties are grafted onto the backbone of poly(acrylic acid) (PAA), forming the PAA-PBA polyelectrolyte. The semi-interpenetrating polymer network (semi-IPN) films composed of PAA-PBA and poly(*N*,*N*-diethylacrylamide) (PDEA) were then synthesized on electrode surface with entrapped horseradish peroxidase (HRP), designated as PDEA-(PAA-PBA)-HRP. The films demonstrated reversible pH-, fructose-, and thermo-responsive on−off behavior toward electroactive probe $K_3Fe(CN)_6$ in its cyclic voltammetric (CV) response. This multiswitchable CV behavior of the system could be further employed to control and modulate the electrochemical reduction of H_2O_2 catalyzed by HRP immobilized in the films with $K_3Fe(CN)_6$ as the mediator in solution. The responsive mechanism of the system was also explored and discussed. The pH-sensitive property was attributed to the electrostatic interaction between the PAA component of the films and the probe at different pH; the thermo-responsive behavior originated from the structure change of PDEA hydrogel component of the films with temperature; the fructose-sensitive property was ascribed to the structure change of the films induced by the complexation between the PBA constituent and the sugar. This smart system could be used as a 3-input logic network composed of enabled OR (EnOR) gates in chemical or biomolecular computing by combining the multiresponsive property of the films and the amplification effect of bioelectrocatalysis and demonstrated the potential perspective for fabricating novel multiswitchable electrochemical biosensors and bioelectronic devices.

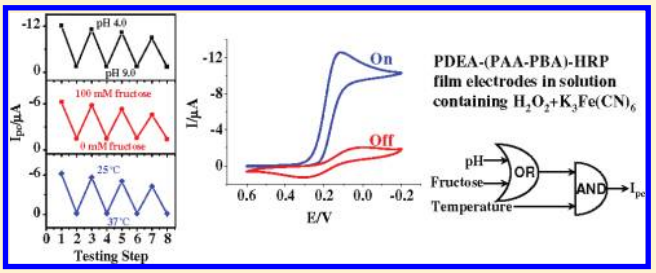

1. INTRODUCTION

Bioelectrocatalysis based on enzymatic reactions can provide an important foundation for fabricating electrochemical biosensors and other biodevices.[1−3] In this regard, the switchable bioelectrocatalysis induced by external stimuli has attracted great interest among researchers in recent years because the reversible activation/deactivation of bioelectrocatalysis by external stimuli not only finds its application in controllable biosensors but also presents the basis for information storage, data processing, and signal amplification.[4−6] Various stimuli have been used to realize switchable bioelectrocatalysis based on enzymes, including pH, temperature, salt, electric field, light, magnetic field, and specific chemicals.[7−12] Great progress has been achieved in this area, and the multiple stimuli-triggered bioelectrocatalysis based on enzymatic reactions has also been reported by our group.[7,9,13,14] However, the development of multiresponsive bioelectrocatalysis is still a task of great challenge. The multiple stimuli-sensitive system demonstrates obvious advantages over the single stimulus-sensitive one since it can add new dimensions and complexity to bioelectrocatalysis, which is more like the real biosystem; it can also open up a new opportunity in some research area, such as the logic gates in chemical and/or biomolecular computing.[15,16]

In recent years, smart interfaces whose electric charge, solubility, volume, structure or conformation, and other properties can be reversibly manipulated dramatically by external stimuli have attracted a great deal of attention.[17−20] Among various intelligent surfaces, multisensitive systems have aroused special interest because in real biological processes, different external stimuli may simultaneously induce the same response including the alteration of protein conformation, the gating of ions across a cell membrane, the change of the membrane permeability, and the on−off of biocatalytic reactions involving enzymes. Impressive results have been achieved in this direction, and various multiresponsive systems have been reported.[21−26] From the point of view of mechanism, the strategies of constructing this kind of system are different. Some specific homopolymers such as poly(*N*-isopropylacrylamide) (PNIPAm) can change their conformation, volume, or other properties with two or more different stimuli because of their unique structures and intrinsic characters.[9,14,23] However, the number of this type of homopolymers is very limited. A more general strategy to create multisensitive materials is to combine two or more different single stimulus-responsive polymer units together. The polymerization of copolymers is usually used for this purpose.[27−30] For example, in the report of

Received: October 11, 2011
Revised: January 11, 2012
Published: January 12, 2012

   dx.doi.org/10.1021/jp209788g | J. Phys. Chem. B 2012, 116, 1700−1708

Li and his co-workers,[28] two monomers, *N*-isopropylacrylamide (NIPAm) and acrylic acid (AA), were electrochemically polymerized into the P(NIPAm-co-AA) copolymer films on the electrode surface. The hydrogel films combined the thermo- and salt-responsive property of PNIPAm with the pH-sensitive behavior of PAA and demonstrated the reversible thermo-, pH-, and salt-responsive on−off behavior toward electroactive probe $Fe(CN)_6^{3-/4-}$ in its cyclic voltammetric (CV) response. Another strategy to design the multiresponsive surfaces is called "binary architecture".[31] For instance, in our recent report,[7] the films that combined pH-sensitive inner layer-by-layer films of concanavalin A and dextran with thermo- and salt-responsive outer poly(*N*,*N*-diethylacrylamide) (PDEA) hydrogel films containing horseradish peroxidase (HRP) were successfully prepared on the electrode surface. The reversibly switchable electrochemical reduction of H_2O_2 catalyzed by HRP in the films and mediated by $K_3Fe(CN)_6$ in solution could be simultaneously triggered and modulated by pH, temperature, and sulfate concentration in solution. Another choice to realize multitriggered interfaces is the synthesis of interpenetrating polymer network (IPN) or semi-IPN materials.[24,25,32,33]

IPNs are a class of polymer blends in which typically two components are polymerized and cross-linked in network form, respectively, and are physically entangled together with each other.[32] IPN hydrogels may possess enhanced mechanical properties compared with individual cross-linked networks due to the entanglements between the two polymer chains. When one of the components of the IPN has a linear instead of a network structure, it is called semi-IPN.[32] Since there is no chemical bonding between the two components in IPNs or semi-IPNs, each component polymer usually retains its own property while the proportion of each polymer can be varied independently. Thus, IPNs or semi-IPNs prepared with two single stimulus-responsive polymers have been employed to construct the multiple stimuli-responsive interfaces.[24,25,32−34] For example, Chen et al. prepared semi-IPN hydrogel particles composed of PNIPAm and chitosan (CS) by inverse suspension polymerization, which showed the reversible change of swelling that was sensitive to both temperature and pH, and the lower critical solution temperature (LCST) of PNIPAm/CS semi-IPN did not shift compared with the pure PNIPAm.[35] However, to the best of our knowledge, the multiresponsive bioelectrocatalysis based on semi-IPN films has not been reported until now.

Phenylboronic acid (PBA) and its derivatives can rapidly and reversibly form a covalent bond with various cis-diol compounds such as sugars by generating five- or six-membered cyclic boronate ester complexes under mild ambient conditions.[36,37] In our previous work,[38] the linear PAA-PBA polyelectrolyte was synthesized by grafting PBA moieties onto the backbone of PAA through the condensation reaction. In PAA-PBA, except for a large fraction of PBA moieties, a considerable amount of free carboxylic acid groups remained, and their protonation would be sensitive to surrounding pH. PDEA is a type of *N*-substituted polyacrylamide and exhibits a reversible and thermo-sensitive phase transition in aqueous solution at the LCST of around 31 °C.[39−41] When the surrounding temperature is below its LCST, PDEA adopts an expanded coil conformation, whereas above the LCST, PDEA takes a shrunken and compact globule structure. In addition, the PDEA hydrogels are also sensitive to the identity and concentration of salts added in solution, and the same phase transition from the extended coil conformation to the compact globule state can be induced by the specific ions with appropriate concentration.[42,43] The thermo- and salt-sensitive behavior of PDEA, the sugar-recognition property of PBA, and the pH-responsive property of PAA-PBA have been reported previously, respectively. However, the synthesis of semi-IPN films combining PAA-PBA and PDEA units together and the study of the corresponding multiple stimuli-responsive properties have not been reported up to now.

In the present work, semi-IPN films composed of PAA-PBA and PDEA with entrapped HRP were synthesized on the electrode surface with a simple one-step polymerization method, designated as PDEA-(PAA-PBA)-HRP. The pH-, fructose-, and thermo-sensitive CV response of $K_3Fe(CN)_6$ at the film electrodes was realized. The temperature and pH are the most important factors in the study of biochemical and biomedical systems. Sugar sensitive materials and interfaces have become particularly important these days because of their potential applications in the development of biomaterials and drug delivery systems.[44] Herein, fructose was chosen as a typical sugar mainly because the complexation of fructose with PBA moiety was more stable than that of other sugars including glucose.[45] This multiswitchable CV behavior of the probe for the films could be further employed to control and modulate the electrochemical reduction of H_2O_2 catalyzed by HRP immobilized in the films and mediated by $K_3Fe(CN)_6$ in solution. The mechanism of the multiply switchable properties of the films toward the probe was also explored and discussed by a series of comparative experiments. The present work provides a novel and convenient model to realize multisignal switchable bioelectrocatalysis and also some unique logic gates that may be used in chemical/biomolecular computing.[15,16] This may open up a new way to develop multiresponsive electrochemical biosensors based on enzymatic reactions and bioelectronic devices based on logic networks so that some biomedical problems may be solved. Nevertheless, we have to point out that the present work represents only the proof of the concept at this stage. A lot of theoretical and experimental works will be needed before the practical applications of the system.

2. EXPERIMENTAL SECTION

2.1. Reagents. Poly(acrylic acid) (PAA, MW ≈ 100 000, 35 wt % solution in water), 3-aminophenyl-boronic acid hemisulfate salt (APBA), 4-(2-hydroxyerhyl) piperazine-1-ethanesulfonic acid (HEPES, 99.5%), *N*-hydroxysulfosuccinimide sodium salt (NHS), 1-(3-dimethylaminopropyl)-3-ethylcarbodiimide hydrochloride (EDC), chitosan (CS, the degree of deacetylation is more than 85%, MW ≈ 200 000), horseradish peroxidase (HRP, E.C. 1.11.1.7, type II, MW ≈ 44 000, 250 000 units g^{-1}), 1,1′-ferrocenedicarboxylic acid ($Fc(COOH)_2$), hexaammineruthenium(III) chloride ($Ru(NH_3)_6Cl_3$), ferrocenemethanol (FcOH), *N*,*N*′-methylenebisacrylamide (BIS), and *N*,*N*,*N*′,*N*′-tetramethylethylenediamine (TEMED) were purchased from Sigma−Aldrich. *N*,*N*-Diethylacrylamide (DEA) was purchased from TCI. Sodium persulfate ($Na_2S_2O_8$) was purchased from Aladdin Reagents. Fructose was obtained from Tianjin Bodi Chemical Engineering Plant. Sodium sulfate (Na_2SO_4), potassium ferricyanide ($K_3Fe(CN)_6$), and hydrogen peroxide (H_2O_2, 30%) were obtained from Beijing Chemical Engineering Plant. The dilute H_2O_2 aqueous solutions were freshly prepared before being used. All other reagents were of analytical grade. Buffer solutions were usually Britton-Robinson buffers at pH 3.0−10.0 containing 0.1 M NaCl, and the pH was

dx.doi.org/10.1021/jp209788g | J. Phys. Chem. B 2012, 116, 1700−1708

adjusted to the desired value with dilute HCl or NaOH solutions. All solutions were prepared with water purified twice by ion exchange and subsequent distillation.

PAA-PBA polyelectrolyte was synthesized by reaction between PAA and APBA in the presence of NHS and EDC by grafting PBA moieties onto the backbone of PAA, and the process was described in detail in our previous work.[38]

2.2. Preparation of PDEA-(PAA-PBA)-HRP Films on Electrodes. Prior to coating, basal plane pyrolytic graphite (PG, Advanced Ceramics) electrodes (geometric area 0.16 cm^2) were abraded with metallographic sandpapers of 320 grits while flushed with water. The electrodes were then ultrasonicated in water for 30 s and dried in air. The PG electrodes were then immersed in 1 mg mL^{-1} CS solutions at pH 5.0 for 20 min to adsorb positively charged CS as the precursor layer. PDEA hydrogel films containing PAA-PBA and HRP, designated as PDEA-(PAA-PBA)-HRP, were prepared on the surface of PG/CS according to the polymerization procedure reported in the literature[46−48] with some modification. In brief, the PG/CS electrodes were placed in a sealed bottle under a high-purity N_2 atmosphere for at least 10 min, and 5 μL of the pregel solution was then cast on the PG/CS surface via a syringe. Herein, after optimization, the typical pregel solution contained 2 mg mL^{-1} PAA-PBA, 2 mg mL^{-1} HRP, 0.5 M DEA monomer, 1.5 mg mL^{-1} BIS cross-linker, 0.4 mg mL^{-1} $Na_2S_2O_8$ initiator, and 0.46 mg mL^{-1} TEMED accelerator, and the solution was freshly prepared and deaerated with N_2 before being cast. The PDEA-(PAA-PBA)-HRP hydrogel films were then formed on the surface of PG/CS in about 6−8 min. During the whole polymerization process, the N_2 atmosphere was kept in the sealed bottle. The formed film electrodes were then immersed in water for about 10 min to remove the unreacted chemicals. The thickness of the films was controlled by the amount of the pregel solution cast on the PG/CS surface. A larger amount of pregel solution would lead to thicker films. Considering the operating convenience and that the CV response of $K_3Fe(CN)_6$ would be slower at the thicker film electrode, 5 μL of the pregel solution was used in preparation of PDEA-(PAA-PBA)-HRP films.

2.3. Apparatus and Procedures. A CHI 660B or CHI 660A electrochemical workstation (CH Instruments) was used for electrochemical measurements. A typical three-electrode cell was used with a saturated calomel electrode (SCE) as the reference, a platinum wire as the counter, and the PG disk electrode with films as the working electrode. The solution was purged with high-purity nitrogen for at least 15 min before electrochemical measurements. The nitrogen atmosphere was then kept above the cell for the entire experiment.

The pH measurements were performed with PHSJ-3F pH-meter (Shanghai Precision & Scientific Instruments). The temperature of solutions in the cell was controlled by an HH-S thermostatic bath (Zhengzhou Greatwall Scientific) with precision of 0.2 °C. The Fourier-transform infrared (FTIR) spectra were recorded at a resolution of 4 cm^{-1} by Nexus 670 Fourier-transform infrared spectrometer (Nicolet). The thickness of hydrogel films was estimated by stereomicroscopy with a Stereo Discovery V12 stereomicroscope equipped with an AxioCam digital camera (Zeiss).

Scanning electron microscopy (SEM) was performed using an S-4800 scanning electron microscope (Hitachi) with an acceleration voltage of 3 kV. The PDEA-(PAA-PBA)-HRP films assembled on PG/CS electrodes were used as the SEM sample. The samples after being treated with different pH, temperatures, and fructose or Na_2SO_4 concentrations were transferred into liquid nitrogen immediately to "freeze" the structure, followed by freeze-drying in an FD-3 freeze drier (Beijing Boyikang Experimental Instrument) for 48 h until all water in the films was sublimed. Before SEM imaging, the sample surface was coated by thin platinum films with an E-1045 sputtering coater (Hitachi).

3. RESULTS AND DISCUSSION

3.1. Characterization of PDEA-(PAA-PBA)-HRP Films. PDEA-(PAA-PBA)-HRP semi-IPN films on PG/CS electrodes were polymerized by radical cross-linking method mainly according to the procedure reported by the literature[46−48] with some modification. The formation of PDEA-(PAA-PBA)-HRP films was confirmed by FTIR spectroscopy in comparison with the pure DEA, PDEA, PAA-PBA, and HRP samples (Supporting Information, Figure S1), and all characteristic IR peaks of those five samples are summarized in the Supporting Information Table S1 according to the literature.[49−52] The characteristic C═C stretching band ($\nu_{C=C}$) at 1609 cm^{-1} observed for DEA monomer was not detected for PDEA and PDEA-(PAA-PBA)-HRP, indicating that the DEA monomer is polymerized into PDEA in these two samples. The C−H stretching vibration bands of $-CH_3$ and $-CH_2-$ (ν_{C-H}) groups at 2970, 2934, and 2875 cm^{-1} for PDEA were also detected for PDEA-(PAA-PBA)-HRP, confirming the formation of PDEA in the films. The synthesis and characterization of PAA-PBA polyelectrolyte was described in detail in our previous work,[38] and the fraction of the carboxylic acid groups in PAA that had been cross-linked with PBA in the PAA-PBA was estimated to be 41%. The characteristic amide II band at 1552 cm^{-1}, the typical B−O stretching peak (ν_{B-O}) at 1340 cm^{-1}, and the characteristic phenyl ring bands at 1490 and 1440 cm^{-1} for PAA-PBA were also observed for PDEA-(PAA-PBA)-HRP. The characteristic C═O stretching band ($\nu_{C=O}$) at 1637 cm^{-1} for pure PDEA and at 1666 cm^{-1} for PAA-PBA merged into one peak at 1655 cm^{-1} for PDEA-(PAA-PBA)-HRP. All of these suggest that the PAA-PBA polyelectrolyte keeps its original form in the PDEA-(PAA-PBA)-HRP hydrogel and is not influenced by the polymerization of PDEA. Thus, the PDEA-(PAA-PBA)-HRP films could be considered to be semi-IPN hydrogel films. The HRP in the films could not be detected by IR spectroscopy since the typical absorption peaks of HRP such as amide I ($\nu_{C=O}$ 1656 cm^{-1}) and II (1546 cm^{-1}) bands were overlapped by those of PDEA and PAA-PBA, respectively, and the amount of HRP in the films was relatively small.

CV with $K_3Fe(CN)_6$ as the electroactive probe was used to confirm the formation of PDEA-(PAA-PBA)-HRP films on electrodes. In pH 9.0 buffers, $K_3Fe(CN)_6$ displayed a well-defined and nearly reversible CV peak pair at about 0.17 V at bare (Supporting Information, Figure S2, curve a) and CS film (Figure S2, curve b) electrodes. After PDEA-(PAA-PBA)-HRP films were formed on the CS film electrodes, the CV response of the probe was severely suppressed (Figure S2, curve d), indicating that a barrier is formed on the electrode surface which hinders the probe from reaching the electrode surface and exchanging electrons with the underlying PG electrodes.

3.2. pH-Sensitive Behavior of PDEA-(PAA-PBA)-HRP Films toward $K_3Fe(CN)_6$. The CV response of $K_3Fe(CN)_6$ at PDEA-(PAA-PBA)-HRP film electrodes at 25 °C was very sensitive to the solution pH (Figure 1A). At pH 4.0, for instance, the probe showed a quasi-reversible CV peak pair with quite large peak heights. However, the peaks decreased

dx.doi.org/10.1021/jp209788g | J. Phys. Chem. B 2012, 116, 1700−1708

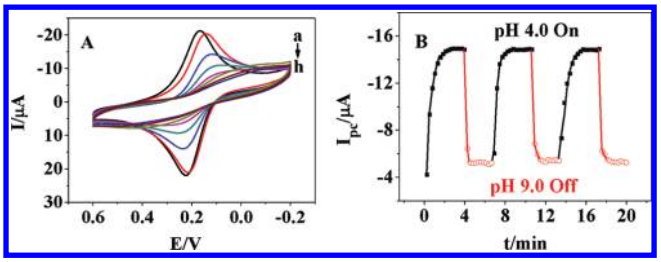

Figure 1. (A) CVs of 1.0 mM $K_3Fe(CN)_6$ at 0.1 V s^{-1} and 25 °C for PDEA-(PAA-PBA)-HRP films in buffers at pH (a) 3.0, (b) 4.0, (c) 5.0, (d) 6.0, (e) 7.0, (f) 8.0, (g) 9.0, and (h) 10.0. (B) Variation of CV I_{pc} with immersion time (t) in solution when pH was switched between pH 4.0 (black square) and 9.0 (red circle) for the same PDEA-(PAA-PBA)-HRP films.

drastically when pH was increased, accompanied by the increase of the peak separation (ΔE_p) (Supporting Information, Figure S3). At pH ≥ 9.0, the CV response could even hardly be observed. This pH-sensitive CV behavior of $K_3Fe(CN)_6$ should be related to the films, since in the control experiment, the CV behavior of $K_3Fe(CN)_6$ at bare PG electrodes was essentially pH-independent. By defining the CV reduction peak current of $K_3Fe(CN)_6$ (I_{pc}) at pH 4.0 for the films as the on state and that at pH 9.0 as the off state, the pH-triggered on−off property of the system was quite reversible. By switching the film electrode in the probe solutions between pH 4.0 and 9.0, the corresponding CV I_{pc} could be changed periodically between a considerably high value and a very small one for many times with the response time of about 2 − 3 min (Figure 1B).

Typically, there are two types of mechanism for pH-sensitive permeation behavior of polyelectrolyte films toward probes. One is mainly controlled by the structure change of films with surrounding pH,[53,54] and the other is mainly tuned by the electrostatic interaction between probes and films, where the surface charge of films can be modulated by external pH.[55−57] To explore the possible change of film structure induced by environmental pH, the surface morphology of PDEA-(PAA-PBA)-HRP films was examined by SEM after the films were treated with pH 4.0 and 9.0 solutions, respectively (Figure 2, panels A and B). With the same magnification, the films that had been treated with pH 4.0 and 9.0 buffers showed no substantial difference in their surface topography, suggesting that the structure of the films is not very sensitive to the environmental pH at least with the present magnification. Moreover, the average thickness of the films at pH 4.0 (208 μm) estimated by stereomicroscopy was nearly the same as that at pH 9.0 (209 μm) (Table 1). Consequently, the pH-sensitive CV on−off property of PDEA-(PAA-PBA)-HRP films toward $K_3Fe(CN)_6$ should be most probably attributed to the electrostatic interaction between them.

To identify which components plays a key role in deciding the pH-sensitive behavior of the PDEA-(PAA-PBA)-HRP films, the PDEA-HRP films containing no PAA-PBA were also polymerized on PG/CS electrode surface, and the CV behavior of $K_3Fe(CN)_6$ was tested at different pH. The results showed that there was no substantial difference in CV response between pH 4.0 and 9.0 for PDEA-HRP films (Supporting Information, Figure S4), indicating that the pH-sensitive property of PDEA-(PAA-PBA)-HRP films toward $K_3Fe(CN)_6$ should be mainly attributed to the PAA-PBA constituent and have little relationship with PDEA component. This is also supported by comparison of CVs of the probe at pH 9.0

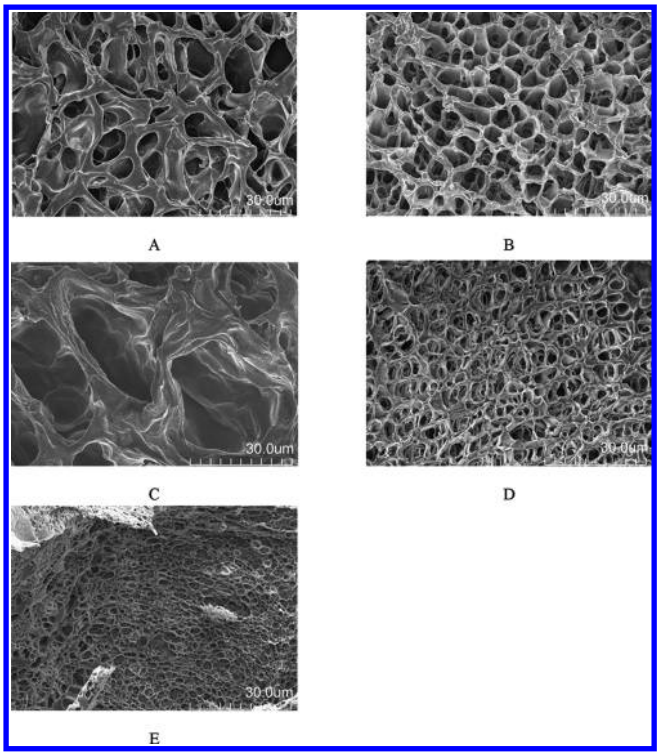

Figure 2. SEM top views of PDEA-(PAA-PBA)-HRP films assembled on PG/CS surface after the films were treated with 1.0 mM $K_3Fe(CN)_6$ buffers for 5 min at (A) pH 4.0 and 25 °C, (B) pH 9.0 and 25 °C, (C) pH 9.0 and 25 °C containing 100 mM fructose, (D) pH 9.0 and 37 °C containing 100 mM fructose, and (E) pH 9.0 and 25 °C containing 100 mM fructose and 0.5 M Na_2SO_4.

Table 1. Average Thickness of PDEA-(PAA-PBA)-HRP Films Estimated by Stereomicroscopy under Different Conditions

conditions	average thickness/μm
pH 4.0 and 25 °C	208 ± 23
pH 9.0 and 25 °C	209 ± 18
pH 9.0 and 25 °C containing 100 mM fructose	237 ± 28
pH 9.0 and 37 °C containing 100 mM fructose	145 ± 20
pH 9.0 and 25 °C containing 100 mM fructose and 0.5 M Na_2SO_4	147 ± 15

between PDEA-HRP and PDEA-(PAA-PBA)-HRP films, where the CV response of the latter (Figure S2, curve d) was much smaller than that of the former (Figure S2, curve c).

The charge situation of the PAA-PBA constituent of the films is sensitive to environmental pH, especially for the PAA moiety.[38] At pH 9.0, PAA carries negative charges because pK_a of PAA is at about 6.0,[58−60] which would result in a strong electrostatic repulsion between PAA-PBA and $Fe(CN)_6^{3-}$ and lead to the very small CV response. In contrast, at pH 4.0, the PAA-PBA carries no charge since both PAA and PBA (pK_a = 8.9[61,62]) would be protonated. Without the electrostatic repulsion, the probe would diffuse through the films more easily, leading to the quite large CV response.

To support this speculation, other electroactive probes with different charges were examined by CV for the films at different pH. The negatively charged $Fc(COOH)_2$[63] demonstrated the on state at pH 4.0 and the off state at pH 9.0 for the films (Supporting Information, Figure S5A), in good agreement with

dx.doi.org/10.1021/jp209788g | J. Phys. Chem. B 2012, 116, 1700−1708

negatively charged $K_3Fe(CN)_6$. However, the positively charged $Ru(NH_3)_6Cl_3$ showed pH-sensitive property for the films with the opposite direction (Figure S5B). The CV response of neutral FcOH was essentially pH-independent and demonstrated quite large CV peaks at both pH 4.0 and 9.0 (Figure S5C). All of these results suggest that it is the electrostatic interaction between the PAA-PBA component of the films and probes that controls the pH-sensitive CV on−off property of the system.

3.3. Fructose-Sensitive Behavior of PDEA-(PAA-PBA)-HRP Films. The CV response of $K_3Fe(CN)_6$ at the PDEA-(PAA-PBA)-HRP film electrodes was also sensitive to the concentration of fructose in solution at pH 9.0 (Figure 3). In

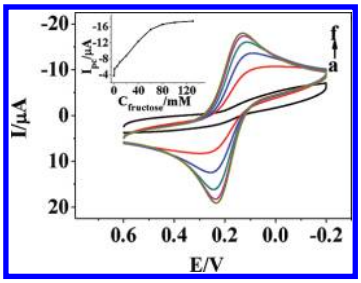

Figure 3. CVs of 1.0 mM $K_3Fe(CN)_6$ for PDEA-(PAA-PBA)-HRP films at 0.1 V s^{-1} and 25 °C in pH 9.0 buffers containing (a) 0, (b) 20, (c) 40, (d) 60, (e) 80, and (f) 100 mM fructose. Inset: dependence of CV I_{pc} on the concentration of fructose.

pH 9.0 buffers containing no fructose, the CV response of the probe was very small and the system was at the off state. However, the addition of fructose in solution led to the dramatic increase of the CV peaks, and the CV I_{pc} increased with fructose concentration up to 80 mM and then tended to level off (Figure 3, inset). If defining the CV response of the probe in buffers at pH 9.0 containing 100 mM fructose for the films as the on state, the CV on−off behavior was reversible and could be repeated for many times when the fructose concentration was switched between 100 and 0 mM with the response time of about 5 min (Supporting Information, Figure S6).

It is well-known that PBA can form complex with various sugars such as fructose.[36,37] The PBA moiety of the PDEA-(PAA-PBA)-HRP films should thus play a key role in the fructose-responsive behavior. To support this speculation, the PDEA-HRP films containing no PAA-PBA were also polymerized on the PG/CS electrode surface, and the CV behavior of $K_3Fe(CN)_6$ was tested with different fructose concentrations. The CV response of the probe demonstrated no essential difference in pH 9.0 buffers with and without fructose at 25 °C for the PDEA-HRP films (Supporting Information, Figure S7), suggesting that the existence of PBA moiety in the films is the precondition for the fructose-sensitive CV behavior of the probe.

PBA moiety in aqueous milieu is in equilibrium between its uncharged and anionic forms with pK_a at about 8.9[61,62] (Supporting Information, Scheme S1). Only the PBA dissociated form can form a stable complex with fructose.[36,37] Therefore, an increase in the concentration of fructose in solution increases the fraction of the total borate anions and decreases the fraction of the uncharged form, making the apparent pK_a become smaller. The addition of fructose makes the PBA moiety transfer from the uncharged state to the negatively charged one, and also from the hydrophobic state to the hydrophilic one with the shift of the equilibrium to the right direction. When this sugar-sensitive property of PBA moiety is combined with the polymer with an amphiphilic character, such as thermo-sensitive PNIPAm, the transition of PBA moiety from hydrophobicity to hydrophilicity would cause the structure change of the polymer and make the polymer swell to a considerable extent.[64,65] PDEA is a kind of amphiphilic polymers with similar structure and thermo-responsive property to PNIPAm. We thus expected that the PDEA-(PAA-PBA)-HRP films would also show sugar-induced structure change and swelling. This speculation was supported by SEM and stereomicroscopy. With the same magnification, the films that had been treated with pH 9.0 buffers containing 100 mM fructose showed much larger aperture of the network in the SEM surface topography than those without fructose (Figure 2, panels B and C). In addition, the average thickness of the films treated with pH 9.0 buffers containing 100 mM fructose estimated by stereomicroscopy (237 μm) was about 13% larger than that treated with no fructose (209 μm) (Table 1). All these results suggest that the fructose-sensitive CV behavior of the probe at PDEA-(PAA-PBA)-HRP film electrodes would be most probably attributed to the structure change of the films induced by fructose. Herein, the PBA moiety acts as the recognition unit and the PDEA as the responsive unit, and the hydrogen-bonding may play an important role in the interactions between the film components, as reported previously for the similar systems.[64,65]

There are two contrary effects when fructose is added in solution for the PDEA-(PAA-PBA)-HRP films. On the one hand, the addition of fructose results in the looser and more swelling structure of the films, making the probe diffuse through the films more easily and leading to the increase of its CV response. On the other hand, the addition of fructose leads to more negative charges on the films and the corresponding increase of electrostatic repulsion with the similarly charged $Fe(CN)_6^{3-}$, resulting in the decrease of its CV response. In our situation, since the addition of fructose in solution caused the increase in CV peaks of the probe for the films, we speculate that the first effect would be predominant. Moreover, while the absolute amount of negative charges of the films would increase with the addition of fructose, the relative charge density might decrease with the increase of the film volume, which would be beneficial to the diffusion of the probe through the films.

The fructose-responsive behavior of the system was also dependent on solution pH, which is clearly demonstrated in the three-dimensional diagram (Figure 4). At pH 4.0, $K_3Fe(CN)_6$

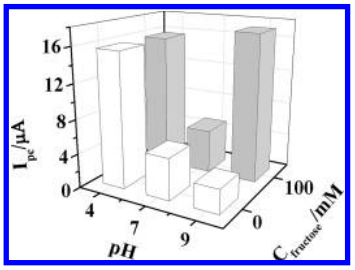

Figure 4. CV I_{pc} of 1.0 mM $K_3Fe(CN)_6$ at 0.1 V s^{-1} and 25 °C in different pH solutions containing different fructose concentrations for the same PDEA-(PAA-PBA)-HRP films.

showed large and similar CV reduction peaks at PDEA-(PAA-PBA)-HRP film electrodes with and without fructose. At pH

dx.doi.org/10.1021/jp209788g | J. Phys. Chem. B 2012, 116, 1700−1708

7.0, the probe demonstrated the same and very small CV response for the films in the absence and presence of fructose. No fructose-sensitive CV behavior of the probe was observed at both pH 4.0 and 7.0. This is understandable since PBA moiety with its pK_a at about 8.9[61,62] takes the uncharged form at pH 4.0 or 7.0 (Scheme S1), and the direct complexation of the uncharged form of PBA with sugar is known to be unstable in water because of its high susceptibility to hydrolysis.[65] Thus, the addition of fructose in solution has little influence on the CV response of the probe at both pH 4.0 and 7.0. However, at pH 9.0, the system displayed the sensitive fructose-responsive behavior (Figure 4) because only in alkaline solution, the charged borate form of PBA moiety of the films can form a stable complex with fructose (Scheme S1).[65]

3.4. Temperature-Sensitive Behavior of PDEA-(PAA-PBA)-HRP Films. The CV response of $K_3Fe(CN)_6$ at PDEA-(PAA-PBA)-HRP film electrodes was sensitive to the environmental temperature with the critical phase transition temperature at about 31 °C (Figure 5), same as the LCST of PDEA.[39−41] When the solution temperature was set below 31 °C, the CV signal of $K_3Fe(CN)_6$ in pH 9.0 buffers containing 100 mM fructose was quite large; however, the peak currents decreased greatly when the temperature was higher than 31 °C. Herein, two typical temperatures, 25 and 37 °C, were selected to study the thermo-responsive on−off property of the films, and the films were at the on state at 25 °C and at the off state at 37 °C (Figure 5, curves a and e). This thermo-sensitive switching behavior of the films was quite reversible and could be repeated for many times between 25 and 37 °C with the response time about 2−5 min (Supporting Information, Figure S8). As a control, the plain PDEA films containing no PAA-PBA in pH 9.0 buffers showed the similar temperature-sensitive behavior (Supporting Information, Figure S9), suggesting that the thermo-sensitive CV behavior of PDEA-(PAA-PBA)-HRP films toward the probe should be attributed to the PDEA component in the films instead of the others. Moreover, the similar position of the LCST of PDEA-(PAA-PBA)-HRP and PDEA films is also a support for the formation of semi-IPN structure for PDEA-(PAA-PBA)-HRP films.[33,40]

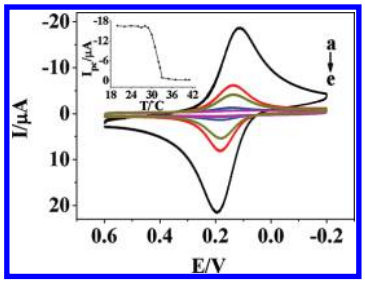

Figure 5. CVs of 1.0 mM $K_3Fe(CN)_6$ for PDEA-(PAA-PBA)-HRP films at 0.1 V s^{-1} in pH 9.0 buffers containing 100 mM fructose at (a) 25, (b) 32, (c) 32.5, (d) 33, and (e) 37 °C. Inset: dependence of CV I_{pc} on the solution temperature (T).

PDEA is a typical thermo-sensitive hydrogel and can undergo the phase transition or conformation change between the coil and globule states in water at its LCST of about 31 °C.[39−41] This can be used to explain the temperature-responsive switching behavior of the PDEA-(PAA-PBA)-HRP films toward $K_3Fe(CN)_6$. At 25 °C, the PDEA component in the films absorbs a great amount of water and takes the swollen and expanded coil state. Thus, the probe can diffuse through the films smoothly and exchange electrons easily with underlying electrodes, displaying the large CV response. When the temperature goes above the LCST such as 37 °C, most of the hydrogen bonds between the PDEA and water molecules are broken, and PDEA takes the shrunken and compact globule structure after the water molecules are squeezed out of the films, leading to the difficulty of the probe going through the films and the corresponding very small CV signal.

The structure change of PDEA-(PAA-PBA)-HRP films with temperature was supported by the results of SEM and stereomicroscopy. The films after treated by pH 9.0 buffers containing 100 mM fructose at 25 °C showed a network structure with many large pores and channels in their surface morphology, whereas the films treated by 37 °C displayed a much more compact network with much smaller pore size (Figure 2, panels C and D). The average film thickness estimated by stereomicroscopy in pH 9.0 buffers containing 100 mM fructose at 25 °C was about 237 μm, much larger than that at 37 °C (145 μm) (Table 1).

It is known that the structure of PDEA hydrogel is also very sensitive to the identity and concentration of salt in solution and the mechanism of the thermo- and salt-sensitive phase transition is similar.[7,42,43] Therefore, we expected that the PDEA-(PAA-PBA)-HRP films should also show salt-sensitive property. Taking Na_2SO_4 as an example, in pH 9.0 buffers containing 100 mM fructose at 25 °C, the increase of Na_2SO_4 concentration in $K_3Fe(CN)_6$ solution resulted in a drastic decrease or even disappearance of the CV peaks of the probe with the critical concentration at about 0.2 M (Supporting Information, Figure S10). 0 and 0.5 M Na_2SO_4 were thus selected as the two typical concentrations to test the Na_2SO_4-sensitive on−off behavior of the system, and the films were at the on state with no sulfate in solution and at the off state when 0.5 M Na_2SO_4 was added (Figure S10A, curves a and f). The addition of 0.5 M Na_2SO_4 in solution led to the transition of the films from the swollen to the compact structure, resulting in the block of the probe to go through the films and the corresponding decrease of CV response. The Na_2SO_4-sensitive structure change of the films was confirmed by SEM (Figure 2, panels C and E) and stereomicroscopy (Table 1). The thermo- and salt-sensitive properties of PDEA-(PAA-PBA)-HRP films were similar to those of the films containing PDEA with the binary architecture in our previous paper[7] because they had the same and common PDEA component.

3.5. Bioactivity of HRP in PDEA-(PAA-PBA)-HRP Films. One of our major concerns for the PDEA-(PAA-PBA)-HRP films was whether the HRP enzyme immobilized in the films could retain its native structure and bioactivity. Since the IR spectroscopic results could not provide convincing evidence that the HRP in the films keeps its original conformation, the biocatalytic activity of HRP in the films toward H_2O_2 was tested by CV with $K_3Fe(CN)_6$ as the electron transfer mediator. When H_2O_2 was added into the $K_3Fe(CN)_6$ solution in pH 9.0 buffers containing 100 mM fructose at 25 °C, in comparison with the system in the absence of H_2O_2, the CV reduction peak of $K_3Fe(CN)_6$ for the films increased, accompanied by the decrease of the oxidation peak (Figure 6). The CV I_{pc} increased initially with the concentration of H_2O_2 in solution up to 0.3 mM and then tended to level off. All these are characteristic of electrochemical reduction of H_2O_2 catalyzed by HRP immobilized in the films and mediated by $K_3Fe(CN)_6$ in solution, and the mechanism can be expressed by the following equations:[66−68]

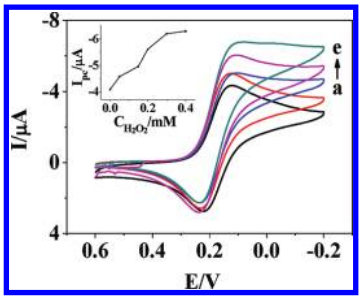

Figure 6. CVs of 1.0 mM $K_3Fe(CN)_6$ at 0.01 V s^{-1} and 25 °C for PDEA-(PAA-PBA)-HRP films in pH 9.0 buffers containing 100 mM fructose and (a) 0, (b) 0.05, (c) 0.15, (d) 0.2, and (f) 0.3 M H_2O_2. Inset: dependence of CV I_{pc} on the concentration of H_2O_2.

$$H_2O_2 + HRP(red) \rightarrow H_2O + HRP(ox)$$

$$HRP(ox) + 2Fe(CN)_6^{4-} \rightarrow HRP(red) + 2Fe(CN)_6^{3-}$$

$$Fe(CN)_6^{3-} + e^- \Leftrightarrow Fe(CN)_6^{4-} \text{ at electrode}$$

where HRP(red) stands for the HRP-Fe(III) form and HRP(ox) usually represents the radical intermediate with oxidation state +5, known as Compound I. The typical electrocatalytic behavior of the system proves that the HRP immobilized in the films retains its bioactivity. To further confirm the function of HRP in the films, the PDEA-(PAA-PBA) films containing no HRP were also polymerized on electrode surface, and as a control, the CV of $K_3Fe(CN)_6$ at the film electrodes was tested in the presence of H_2O_2. No electrocatalytic reduction of H_2O_2 was observed (Supporting Information, Figure S11), suggesting that the HRP enzyme in the films plays a central role in the bioelectrocatalysis of H_2O_2.

3.6. Multiply Sensitive Switching of PDEA-(PAA-PBA)-HRP Films in Bioelectrocatalysis. The pH-, fructose-, and thermo-sensitive CV switching property of PDEA-(PAA-PBA)-HRP films toward $K_3Fe(CN)_6$ inspired us to use this system to control or modulate the electrocatalytic reduction of H_2O_2 by HRP entrapped in the films with these three stimuli. For example, in pH 4.0 solutions containing $K_3Fe(CN)_6$ and H_2O_2 at 25 °C, the films demonstrated a large electrocatalytic reduction peak (Figure 7A, curve a). However, when the films were placed in pH 9.0 buffers containing the same amount of $K_3Fe(CN)_6$ and H_2O_2, the electrocatalytic response became quite small (Figure 7A, curve b). This is because the films become "closed" to the probe at pH 9.0, resulting in the interruption of the catalytic cycles. The bioelectrocatalysis was "open" at pH 4.0 and "closed" at pH 9.0, and this pH-sensitive on−off bioelectrocatalysis for the system could be repeated for at least several cycles by switching the same films in the $K_3Fe(CN)_6$ + H_2O_2 solutions between pH 4.0 and 9.0 (Figure 8, panel A).

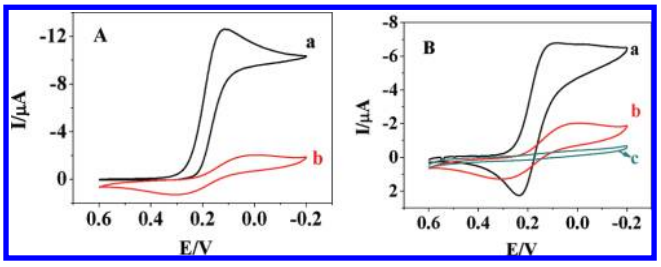

Figure 7. (A) CVs of 1.0 mM $K_3Fe(CN)_6$ at 0.01 V s^{-1} and 25 °C for PDEA-(PAA-PBA)-HRP films in buffers containing 0.4 mM H_2O_2 at (a) pH 4.0 and (b) 9.0. (B) CVs of 1.0 mM $K_3Fe(CN)_6$ at 0.01 V s^{-1} and pH 9.0 for PDEA-(PAA-PBA)-HRP films in buffers containing 0.4 mM H_2O_2 at (a) 25 °C in the presence of 100 mM fructose, (b) 25 °C in the absence of fructose, and (c) 37 °C in the presence of 100 mM fructose.

Similarly, in pH 9.0 buffers containing $K_3Fe(CN)_6$ and H_2O_2 at 25 °C with 100 mM fructose, the bioelectrocatalysis for the films was at the on state (Figure 7B, curve a). When the fructose was absent, however, the system became off (Figure 7B, curve b). The fructose-triggered bioelectrocatalysis of H_2O_2 for the system could also be switched between the on and off states reversibly and repeated for many times (Figure 8, panel B). The reversible temperature-switchable bioelectrocatalysis of H_2O_2 by the films with $K_3Fe(CN)_6$ as the mediator was also observed (Figure 7B, curve c; Figure 8, panel C). With the bioelectrocatalysis, the difference between the on and off states could be amplified.

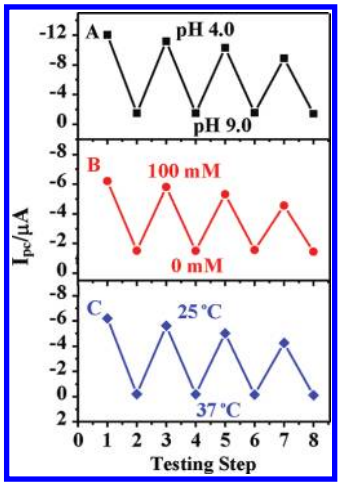

Figure 8. Dependence of CV I_{pc} of 1.0 mM $K_3Fe(CN)_6$ at 0.01 V s^{-1} for PDEA-(PAA-PBA)-HRP films in buffers containing 0.4 mM H_2O_2 (A) on solution pH switched between 4.0 and 9.0 in the absence of fructose, (B) on fructose concentration switched between 100 and 0 mM at 25 °C and pH 9.0, and (C) on solution temperature switched between 25 and 37 °C in pH 9.0 buffers containing 100 mM fructose.

3.7. System Acted as a Logic Gate. The triply switchable bioelectrocatalysis system could be used to construct the 3-input logic gate system. Herein, pH was defined as input A, and pH 9.0 and 4.0 were defined as "**0**" and "**1**" states, respectively. Similarly, for the fructose concentration (input B) and the temperature (input C), 0 mM and 37 °C were defined as "**0**", and 100 mM and 25 °C as "**1**", respectively. The CV I_{pc} of $K_3Fe(CN)_6$ for PDEA-(PAA-PBA)-HRP films in the presence of H_2O_2 acted as output with larger I_{pc} value as "**1**" and smaller one as "**0**" when 3 μA was defined as the threshold. All possible 8 combinations of the 3-input signals were examined for the system, and only three of them (1,1,1; 1,0,1; 0,1,1) resulted in the "**1**" output or the on state while other five (1,0,0; 1,1,0; 0,1,0; 0,0,1; 0,0,0) would lead to the "**0**" output or the off state (Table 2 and Figure 9).

It is worth noticing that the sugar-induced CV on−off behavior of the system could not be observed at pH 4.0 and the films were always at the on state at this pH no matter whether fructose was in the presence or absence (Figure 4). Only at pH

dx.doi.org/10.1021/jp209788g | J. Phys. Chem. B 2012, 116, 1700−1708

Table 2. Truth Table for the 3-Input Logic Gate

input A	input B	input C	output
pH	fructose	temperature	I_{pc}
1	1	1	1
1	0	1	1
0	1	1	1
0	0	1	0
1	1	0	0
0	1	0	0
1	0	0	0
0	0	0	0

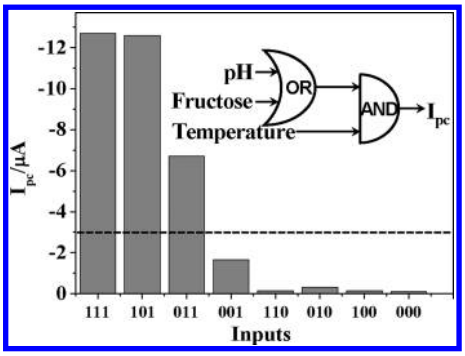

Figure 9. CV I_{pc} of 1.0 mM $K_3Fe(CN)_6$ at 0.01 V s^{-1} for PDEA-(PAA-PBA)-HRP films in buffers containing 0.4 mM H_2O_2 as the output with different inputs. The dashed line marks the threshold. The inset shows the symbolic representation of the EnOR logic gate.

9.0, the fructose-responsive on−off switching of the films could be realized (Figures 3 and 4). It is this unique behavior that leads to the distinctive 3-input truth table (Table 2) and the corresponding bar diagram (Figure 9) in bioelectrocatalysis. These results were consistent with an enabled OR (EnOR) logic gate[69,70] which is enabled by either input A or input B at their "**1**" levels only when the third input (input C) is activated at "**1**" (Figure 9, inset). As we know, this is the first report on a biomolecular EnOR gate constructed on electrode surface.

In fact, the PDEA-(PAA-PBA)-HRP films were also sensitive to the sulfate concentration in solution, as mentioned above (Figure S10), and the sulfate concentration could be used as the fourth input (input D) in the logic network. The truth table of the 4-input system is presented as Supporting Information Table S2 if 0 and 0.5 M of sulfate were defined as "**1**" and "**0**" for input D, respectively. According to the truth table, a new and more complicated logic network could also be constructed (Supporting Information, Figure S12). As expected, the increase of the number of stimuli or inputs would lead to more complicated logic gates or networks with enhanced levels of complexity.

4. CONCLUSIONS

In this work, PAA-PBA polyelectrolyte and DEA monomer are polymerized into PDEA-(PAA-PBA) semi-IPN hydrogel films with entrapped HRP on the surface of PG electrodes by a simple one-step polymerization method with only about 35 min at room temperature. The probe $K_3Fe(CN)_6$ exhibits reversible pH-, fructose-, and temperature-sensitive CV on−off behavior at the film electrodes. It is the integration of several functional moieties or units in one semi-IPN structure that results in multiple stimuli-sensitive responses. The pH-responsive property of the system mainly originates from the electrostatic interaction between the PAA moieties of the films and the probe at different pH; the thermo-sensitive behavior is attributed to the structure change of PDEA hydrogel component with temperature; while the fructose-responsive property is mainly ascribed to the structure alteration of the films induced by the complexation between the PBA constituent and the sugar, where the PBA is the recognition unit and the PDEA is the switching unit. The films can also be used to realize multiply switchable electrochemical reduction of H_2O_2 catalyzed by HRP entrapped in the films and mediated by $K_3Fe(CN)_6$ in solution. The novelty and breakthrough of this study is its first report on multiswitchable bioelectrocatalysis based on semi-IPN hydrogel films and the construction of the unique multi-input biomolecular EnOR logic gate on electrode surface. The bioelectrocatalysis can lead to the great amplification of signal/noise ratio in CV on−off output, which is favorable to the construction of logic networks when combined with the multiresponsive property of the system. While this work represents only the proof of the concept at this stage, it did represent the important progress toward the direction of practical applications. For example, this kind of logic gates may establish a foundation for fabricating a novel type of smart decision-making logic networks which are able to accept many input signals and produce binary outputs in the form of YES/NO so that some biomedical problems may be solved within a single interface in the future.[16]

■ ASSOCIATED CONTENT

Supporting Information

Twelve figures show FTIR of HRP, DEA, PDEA, PAA-PBA and PDEA-(PAA-PBA)-HRP films, CVs of $K_3Fe(CN)_6$ at bare PG, CS, PDEA-HRP and PDEA-(PAA-PBA)-HRP film electrodes in pH 9.0 at 25 °C, influence of pH on CV I_{pc} and ΔE_p of $K_3Fe(CN)_6$ for PDEA-(PAA-PBA)-HRP films at 25 °C, CVs of $K_3Fe(CN)_6$ at PDEA-HRP film electrodes in pH 4.0 and 9.0 buffers at 25 °C, CVs of $Fc(COOH)_2$, $Ru(NH_3)_6Cl_3$, and FcOH at PDEA-(PAA-PBA)-HRP film electrodes in pH 4.0 and 9.0 buffers at 25 °C, dependence of CV I_{pc} of $K_3Fe(CN)_6$ on immersion time in pH 9.0 buffers containing fructose switched between 100 and 0 mM for PDEA-(PAA-PBA)-HRP films at 25 °C, CVs of $K_3Fe(CN)_6$ at PDEA-HRP film electrodes in pH 9.0 buffers containing 0 and 100 mM fructose at 25 °C, dependence of CV I_{pc} of $K_3Fe(CN)_6$ on immersion time when the temperature switched between 25 and 37 °C for PDEA-(PAA-PBA)-HRP films in pH 9.0 buffers containing 100 mM fructose, CVs of $K_3Fe(CN)_6$ for PDEA films in pH 9.0 buffers at 25 and 37 °C, dependence of CV I_{pc} of $K_3Fe(CN)_6$ for PDEA films on the solution temperature in pH 9.0 buffers, CVs of $K_3Fe(CN)_6$ for PDEA-(PAA-PBA)-HRP films in pH 9.0 buffers containing 100 mM fructose and 0, 0.1, 0.2, 0.3, 0.4, and 0.5 M Na_2SO_4 at 25 °C, dependence of CV I_{pc} on the concentration of Na_2SO_4 for PDEA-(PAA-PBA)-HRP films at 25 °C, CVs of $K_3Fe(CN)_6$ at 25 °C in pH 9.0 buffers containing 100 mM fructose and H_2O_2 for PDEA-(PAA-PBA)-HRP and PDEA-(PAA-PBA) films, and the symbolic representation of 4-input logic network. Two tables show assignment of observed IR peaks for different samples and the truth table for the 4-input logic gate. One scheme shows equilibria of PAA-PBA system. This material is available free of charge via the Internet at http://pubs.acs.org.

dx.doi.org/10.1021/jp209788g | J. Phys. Chem. B 2012, 116, 1700−1708

AUTHOR INFORMATION

Corresponding Author

*E-mail: hunaifei@bnu.edu.cn. Tel: (+86) 10-5880-5498. Fax: (+86) 10-5880-2075.

Notes

The authors declare no competing financial interest.

ACKNOWLEDGMENTS

Financial support from the National Natural Science Foundation of China (NSFC 20975015 and 21105004) is acknowledged.

REFERENCES

(1) Scheller, F. W.; Wollenberger, U.; Warsinke, A.; Lisdat, F. *Curr. Opin. Biotechnol.* **2001**, *12*, 35.
(2) Chaubey, A.; Malhotra, B. D. *Biosens. Bioelectron.* **2002**, *17*, 441.
(3) Murphy, L. *Curr. Opin. Chem. Biol.* **2006**, *10*, 177.
(4) Pita, M.; Katz, E. *Electroanalysis* **2009**, *21*, 252.
(5) Willner, I. *Acc. Chem. Res.* **1997**, *30*, 347.
(6) Willner, I.; Katz, E. *Angew. Chem., Int. Ed.* **2000**, *39*, 1180.
(7) Yao, H.; Hu, N. *J. Phys. Chem. B* **2011**, *115*, 6691.
(8) Tam, T. K.; Ornatska, M.; Pita, M.; Minko, S.; Katz, E. *J. Phys. Chem. C* **2008**, *112*, 8438.
(9) Song, S.; Hu, N. *J. Phys. Chem. B* **2010**, *114*, 5940.
(10) Katz, E.; Willner, I. *J. Am. Chem. Soc.* **2003**, *125*, 6803.
(11) Blonder, R.; Katz, E.; Willner, I.; Wray, V.; Buckmann, A. F. *J. Am. Chem. Soc.* **1997**, *119*, 11747.
(12) Hirsch, R.; Katz, E.; Willner, I. *J. Am. Chem. Soc.* **2000**, *122*, 12053.
(13) Liang, Y.; Song, S.; Yao, H.; Hu, N. *Electrochim. Acta* **2011**, *56*, 5166.
(14) Song, S.; Hu, N. *J. Phys. Chem. B* **2010**, *114*, 11689.
(15) Silva, A. P. D; Uchiyama, S. *Nat. Nanotechnol.* **2007**, *2*, 399.
(16) Wang, J.; Katz, E. *Anal. Bioanal. Chem.* **2010**, *398*, 1591.
(17) Cole, M. A.; Voelcker, N. H.; Thissen, H.; Griesser, H. J. *Biomaterials* **2009**, *30*, 1827.
(18) Nandivada, H.; Ross, A. M.; Lahann, J. *Prog. Polym. Sci.* **2010**, *35*, 141.
(19) Zhang, J.; Han, Y. *Chem. Soc. Rew.* **2010**, *39*, 676.
(20) Mendes, P. M. *Chem. Soc. Rev.* **2008**, *37*, 2512.
(21) Pasparakis, G.; Vamvakaki, M. *Polym. Chem.* **2011**, *2*, 1234.
(22) Jiang, Y. G.; Wan, P.; Smet, M.; Wang, Z.; Zhang, X. *Adv. Mater.* **2008**, *20*, 1972.
(23) Zhang, M.; Liu, L.; Zhao, H.; Yang, Y.; Fu, G.; He, B. *J. Colloid Interface Sci.* **2006**, *301*, 85.
(24) Zhang, J.; Peppas, N. *Macromolecules* **2000**, *33*, 102.
(25) Zhao, Y.; Kang, J.; Tan, T. *Polymer* **2006**, *47*, 7702.
(26) Xia, H.; Xia, F.; Tang, Y.; Guo, W.; Hou, X.; Chen, L.; Hou, Y.; Zhang, G.; Jiang, L. *Soft Matter* **2011**, *7*, 1638.
(27) Dimitrov, I.; Trzebicka, B.; Muller, A. H. E.; Dworak, A.; Tsvetanov, C. B. *Prog. Polym. Sci.* **2007**, *32*, 1275.
(28) Zhou, J.; Wang, G.; Hu, J.; Lu, X.; Li, J. *Chem. Commun.* **2006**, *46*, 4820.
(29) Xia, F.; Ge, H.; Hou, Y.; Sun, T.; Chen, L.; Zhang, G.; Jiang, L. *Adv. Mater.* **2007**, *19*, 2520.
(30) Bousquet, A.; Ibarboure, E.; Papon, E.; Labrugere, C.; Rodriguez-Hernandez, J. *J. Polym. Sci., Part A: Plym. Chem.* **2010**, *48*, 1952.
(31) Fulghum, T. M.; Estillore, N. C.; Vo, C.-D.; Armes, S. P.; Advincula, R. C. *Macromolecules* **2008**, *41*, 429.
(32) Bajpai, A. K.; Shukla, S. K.; Bhanu, S.; Kankane, S. *Prog. Polym. Sci.* **2008**, *33*, 1088.
(33) Wandera, D.; Wickramasinghe, S. R.; Husson, S. M. *J. Membr. Sci.* **2010**, *357*, 6.
(34) Lee, W. F.; Chen, Y. J. *J. Appl. Polym. Sci.* **2001**, *82*, 2487.
(35) Chen, X.; Song, H.; Fang, T.; Bai, J.; Xiong, J.; Ying, H. *J. Appl. Polym. Sci.* **2010**, *116*, 1342.
(36) James, T. D.; Sandanayake, K. R. A. S.; Shinkai, S. *Angew. Chem., Int. Ed.* **1996**, *35*, 1910.
(37) James, T. D.; Shinkai, S. *Top. Curr. Chem.* **2002**, *218*, 159.
(38) Yao, H.; Chang, F.; Hu, N. *Electrochim. Acta* **2010**, *55*, 9185.
(39) Maeda, Y.; Yamamoto, H.; Ikeda, I. *Langmuir* **2001**, *17*, 6855.
(40) Chen, J.; Liu, M.; Liu, H.; Ma, L.; Gao, C.; Zhu, S.; Zhang, S. *Chem. Eng. J.* **2010**, *159*, 247.
(41) Mao, H.; Li, C.; Zhang, Y.; Berbreiter, D. E.; Cremer., P. S. *J. Am. Chem. Soc.* **2003**, *125*, 2850.
(42) Chen, Y.; Liu, M.; Bian, F.; Wang, B.; Chen, S.; Jin, S. *Macromol. Chem. Phys.* **2006**, *207*, 104.
(43) Panayiotou, M.; Freitag, R. *Polymer* **2005**, *46*, 6777.
(44) Miyata, T.; Uragami, T.; Nakamae, K. *Adv. Drug Delivery Rev.* **2002**, *54*, 79.
(45) Shoji, E.; Freund, M. S. *J. Am. Chem. Soc.* **2002**, *124*, 12486.
(46) Panayiotou, M.; Freitag, R. *Polymer* **2005**, *46*, 615.
(47) Ding, X.; Fries, D.; Jun, B. *Polymer* **2006**, *47*, 4718.
(48) Chen, J.; Liu, M.; Liu, H.; Ma, L. *Mater. Sci. Eng., C* **2009**, *29*, 2116.
(49) Smith, B. C. *Infrared Spectral Interpretation: A Systematic Approach*; CRC Press: New York, 1999.
(50) Stuart, B. H. *Infrared Spectroscopy: Fundamentals and Applications*; Wiley: New York, 2004.
(51) Maeda, Y.; Nakamura, T.; Ikeda, I. *Macromolecules* **2002**, *35*, 10172.
(52) Chu, L.; Zou, X.; Knoll, W.; Forch, R. *Surf. Coat. Technol.* **2008**, *202*, 2047.
(53) Motornov, M.; Sheparovych, R.; Katz, E.; Minko, S. *ACS Nano* **2008**, *2*, 41.
(54) Antipova, A. A.; Sukhorukov, G. B. *Adv. Colloid Interface Sci.* **2004**, *111*, 49.
(55) Kang, E. H.; Liu, X.; Sun, J.; Shen, J. *Langmuir* **2006**, *22*, 7894.
(56) Liu, Y. L.; Zhao, M. Q.; Bergbreiter, D. E.; Crooks, R. M. *J. Am. Chem. Soc.* **1997**, *119*, 8720.
(57) Calvo, A.; Yameen, B.; Williams, F. J.; Soler−Illia, G. J.; Azzaroni, O. *J. Am. Chem. Soc.* **2009**, *131*, 10866.
(58) Mittal, K. L. *Acid-Base Interaction: Relevance to Adhesion Science and Technology*; VSP: Utrecht, The Netherlands, 2000; Vol. 2.
(59) Gregor, H. P.; Luttinger, L. B.; Loebl, E. M. *J. Am. Chem. Soc.* **1954**, *76*, 5879.
(60) Laguecir, A.; Ulrich, S.; Labille, J.; Fatin-Rouge, F.; Stoll, S.; Buffer, J. *Eur. Polym. J.* **2006**, *42*, 1135.
(61) Branch, G. E. K.; Yabroff, D. S.; Bettman, B. *J. Am. Chem. Soc.* **1934**, *56*, 937.
(62) Hoare, T.; Pelton, R. *Biomacromolecules* **2008**, *9*, 733.
(63) Song, S.; Hu, N. *J. Phys. Chem. B* **2010**, *114*, 3648.
(64) Qing, G.; Wang, X.; Jiang, L.; Fuchs, H.; Sun, T. *Soft Matter* **2009**, *5*, 2759.
(65) Kataoka, K.; Miyaaki, H.; Bunya, M.; Okana, T.; Sakurai, Y. *J. Am. Soc. Chem.* **1998**, *120*, 12694.
(66) Pan, S.; Arnold, M. A. *Anal. Chim. Acta* **1993**, *283*, 663.
(67) Li, W.; Yuan, R.; Chai, Y.; Zhou, L.; Chen, S.; Li, N. *J. Biochem. Biophys. Methods* **2008**, *70*, 830.
(68) Lu, B.; Smyth, M. R.; Quinn, J.; Bogan, D.; O'Kennedy, R. *Electroanalysis* **1996**, *8*, 619.
(69) Sousa, M.; Castro, B.; Abad, S.; Miranda, M. A.; Pischel, U. *Chem. Commun.* **2006**, *19*, 2051.
(70) Roque, A.; Pina, F.; Alves, S.; Ballardini, R.; Maestri, M.; Balzani, V. *J. Mater. Chem.* **1999**, *9*, 2265.